Preparation of $BaZrO_3$ powders by a spray-drying process

B. Robertz, F. Boschini, A. Rulmont, and R. Cloots[a)]
LCIS, Department of Chemistry, Chemistry Institute B6, University of Liège, Sart Tilman, B-4000 Liège, Belgium

I. Vandriessche and S. Hoste
Department of Inorganic and Physical Chemistry, University Gent, Krijgslaan 281, B-9000 Gent, Belgium

J. Lecomte-Beckers
Department of Metallurgy, University of Liège, Sart Tilman B52, B-4000 Liège, Belgium

(Received 15 July 2002; accepted 18 February 2003)

The potential use of barium zirconate for the manufacture of corrosion-resistant substrates emphasizes the need for a simple, inexpensive, and easily scalable process to produce high-quality powders with well-controlled composition and properties. However, the classical solid-state preparation of barium zirconate leads to an inhomogeneous powder unsuitable for applications in highly corrosive environment. For this paper, the possibility to use the spray-drying technique for the preparation of $BaZrO_3$ powders with a controlled size distribution and morphology was investigated. The influence of the nature and concentration of the precursor solution and the influence of the spray drying step are discussed on the basis of x-ray diffraction, Fourier transform infrared spectroscopy, scanning electron microscopy, and dilatometric measurements.

I. INTRODUCTION

For the past few years, there has been growing interest in the synthesis of high-quality barium zirconate powder. The need for reactive, ultrafine, high-purity powders has triggered the development of soft chemistry processes.[1–10] In fact, the potential use of barium zirconate for the manufacture of corrosion resistant substrates and artifacts[11] (crucibles, high temperature construction elements) emphasizes the need for a simple, inexpensive and easily scalable process to produce high-quality powders with well-controlled composition and properties.

For this paper, a novel method exploiting the advantages of the spray drying process was investigated. The advantages of the use of spray drying to synthesize high-quality ceramics are numerous. The spray-drying technique generally leads to the formation of spherical powder agglomerates, through the drying of sprayed droplets,[12] with better control of homogeneity, particle size, and particle-size distribution. Moreover, the reactivity of the obtained powder is also improved.[13,14]

Particular attention was paid to the influence of the type of barium and zirconium sources and the presence of an organic fuel (oxalic dihydrazide[15]) on the morphology, chemical composition, and sintering behavior of the as-obtained materials.

II. EXPERIMENTAL

The experimental procedure involves several steps: preparation of the mixed precursor solutions of barium and zirconium, spray drying of the solutions, and calcination of the spray-dried powders, followed by characterization of the end products.

A. Preparation of the precursor solutions

The precursor solutions were prepared from different barium and zirconium sources with 1:1 stoichiometry. Table I summarizes the compositions of the different solutions thus prepared. An organic fuel (oxalyl dihydrazide $NH_2NHCOCONHNH_2$) was added in SD6 and SD7 cases only (15 wt.% of the total salt weight). The addition of an organic fuel to the solution could lead to the formation of barium zirconate at a temperature much lower than that required for the classical solid state reaction route. Nitrate metal salts are commonly used because of their oxidizing character; the organic fuel acts as a reducing agent. Practically, solutions containing the metal nitrates and the organic fuel become relatively viscous. A gel-like solution is then spray dried. Because of

a)Address all correspondence to this author.
e-mail: rcloots@ulg.ac.be

TABLE I. Summary of the compositions of the starting solutions.

Denomination	Barium source	Zirconium source	Concentration in each ion (mol/l)	$(NH_2NHCO)_2$
SD1	$Ba(NO_3)_2$	$ZrO(NO_3)_2 \cdot 5H_2O$	0.15	No
SD2	$BaCl_2 \cdot 2H_2O$	$ZrOCl_2 \cdot 8H_2O$	0.5	No
SD3	$Ba(Ac)_2$	"$ZrOCO_3$" + HAc	0.5	No
SD4	$Ba(NO_3)_2$	$ZrOCl_2 \cdot 8H_2O$	0.3	No
SD5	$Ba(NO_3)_2$	"$ZrOCO_3$" + HNO_3	0.15	No
SD6	$Ba(NO_3)_2$	$ZrO(NO_3)_2 \cdot 5H_2O$	0.15	15%
SD7	$Ba(NO_3)_2$	"$ZrOCO_3$" + HNO_3	0.15	15%

the vigorous nature of the reaction, only a small amount of fuel, corresponding to 15 wt.% with respect to the total weight of the metal salts, was added. It is thus very important to keep in mind the relatively high viscosity of the parent solution when an organic fuel is used, to compare the results with respect to the other cases. Viscosity measurements were not performed on the precursor solutions because only two cases have to be considered: high-viscosity and low-viscosity precursor solutions.

The first set of solutions was obtained by mixing an aqueous solution of $Ba(NO_3)_2$ with a solution of $ZrO(NO_3)_2 \cdot 5H_2O$ to reach a final concentration of 0.15 mol/dm^3 for each cation (SD1).

The second solution (SD2) was obtained by the dissolution of $BaCl_2 \cdot 2H_2O$ and $ZrOCl_2 \cdot 8H_2O$ to obtain a final concentration of 0.25 mol/dm^3 for each cation.

Solution SD3 was made of a mixture of the acetate salts of both ions. Basic zirconium carbonate was dissolved in 50 ml of a 0.8 mol/dm^3 acetic acid to which an appropriate amount of barium acetate was added to obtain 0.5 mol/dm^3 for each cation. The exact formula of the basic zirconium carbonate hydrate is not known, but it contains 1.44 mol ZrO_2 per mole of compound as determined by thermogravimetric analysis. The carbonate is easily dissolved in acetic acid as a complex anion $[HOOZr(OOCCH_3)_2 \cdot 2H_2O]^-$ corresponding to the diacetatozirconic acid. This compound cannot be isolated in crystalline form. Upon evaporation, a polymerization reaction by the formation of oxygen bridges between the zirconium atoms takes place and an amorphous solid precipitates.[16]

$Ba(NO_3)_2$ and $ZrOCl_2 \cdot 8H_2O$ were used as Ba and Zr sources for solution SD4. The salts were dissolved in deionized water to obtain a 0.3 mol/dm^3 solution.

For solution SD5, the basic zirconium carbonate was dissolved in 30 ml 3 mol/dm^3 HNO_3. This was added to 170 ml $Ba(NO_3)_2$ solution. The solution was 0.15 mol/dm^3 in each cation.

An organic fuel, $NH_2NHCOCONHNH_2$, was added under gentle heating conditions to solutions SD1 and SD5. These solutions are labeled SD6 and SD7, respectively. The fuel content corresponded to 15 wt.% with respect to the total weight of the barium and zirconium salts.

In all cases, clear and stable solutions could be spray dried, even if the solutions containing the organic fuel had a higher viscosity.

A summary of the synthesis conditions is also provided in Table I.

B. Spray drying, calcination, and characterization.

Spray drying through a concurrent flow atomization process for the precursor solutions was performed on a Büchi 190 instrument using a 0.5 mm nozzle, an inlet AU2 temperature of 225 °C, and a liquid feed rate of 5 ml/min. The outlet temperature during spraying was 160 °C. The spray drying was performed in air, using a flow rate of 800 normal l/h. All the dried powders were simultaneously treated in a muffle furnace. Thermogravimetric analysis (TGA) and differential scanning colonmetry (DSC) were performed in air at a heating rate of 10 °C/min using a Netzsch device. X-ray diffraction analysis (XRD; AU2 Siemens D-5000) was carried out on the powders calcined at the different temperatures (500 and 600 °C) for AU2 2 h. The progress of the reaction was also followed by Fourier transform infrared (FTIR) spectroscopy of powders in KBr disks. The morphology of the powders was studied by high-resolution scanning electron microscopy. A sintering study was conducted using a Netzsch dilatometer (DIL 402C) with a heating rate of 3 °C/min from room temperature to 1450 °C. Rods 25 mm long were isostatically pressed. The can consisted of a silicone tube sealed with a cap. The tube was air evacuated before pressing to avoid cracking due to entrapped gases. A pressure of 220 MPa was applied for 10 min.

III. RESULTS AND DISCUSSION

A. Structural characterization

Precipitation of barium nitrate crystals was clearly observed in the as-sprayed SD1 and SD4 solutions [Fig. 1(a)]. The as-sprayed SD3 solution was amorphous Fi as specified in Sec. II. A. It corresponds to the polymerization through water evaporation of the anion of the diacetatozirconic acid by the formation of oxygen bridges

between the zirconium atoms. Only barium chloride with poor crystallinity was observed in the as-sprayed SD2 solution [Fig. 1(b)]. Only a few reflection peaks can be identified. A mathematical treatment was applied to extract the background contribution, resulting, in the case of a poor crystalline material, in a very low-intensity x-ray signal. Zirconium species are generally not detected on the x-ray patterns. Moreover, zirconium ions precipitated from the solution have a tendency to form a hydrated amorphous zirconia phase, thus not easily detected by XRD. On the other hand, barium compounds give high intensity XRD patterns due to the high atomic diffusion factor for barium, often masking the other species present in the powder. In Fig. 1(a), however, the most intense peak of crystalline $ZrO(NO_3)_2 \cdot 5H_2O$ is detected. This peak is no longer present when the basic zirconium carbonate dissolved in diluted nitric acid (SD5) is used instead of zirconyl nitrate hydrate. In Fig. 1(b), the x-ray reflection peaks correspond to orthorhombic $BaCl_2$ and $BaCl_2 \cdot H_2O$. The most intense peaks of barium zirconate and orthorhombic or tetragonal zirconia have the same value of diffraction angle at 30° (2θ).[17] Neither the presence of barium zirconate nor the presence of zirconia could be inferred from the x-ray patterns of the as-spray-dried powders.

1. $BaZrO_3$ from nitrate solution SD1

The TGA/DSC curve of the spray-dried mixture of nitrates is presented in Fig. 2. The broad peak below 200 °C corresponds to the loss of residual water. A stable weight compound is obtained at 800 °C, and it corresponds to barium zirconate slightly contaminated with barium carbonate. The formation of the barium zirconate phase appears as an endotherm centered around 600 °C. The decomposition of $Ba(NO_3)_2$ in the presence of ZrO_2 might occur at a temperature lower than that of a pure $Ba(NO_3)_2$, which takes place between 600 and 800 °C. $ZrO(NO_3)_2$ decomposes at a temperature closer to 400 °C, as has been deduced from thermogravimetric measurements. The lower decomposition temperature of the zirconyl nitrate might also be responsible for the low formation temperature of barium zirconate from nitrates. The XRD patterns of the mixture heated for 2 h at 500 and 600 °C, respectively, are shown in Fig. 3. They confirm the formation of barium zirconate between 500 and

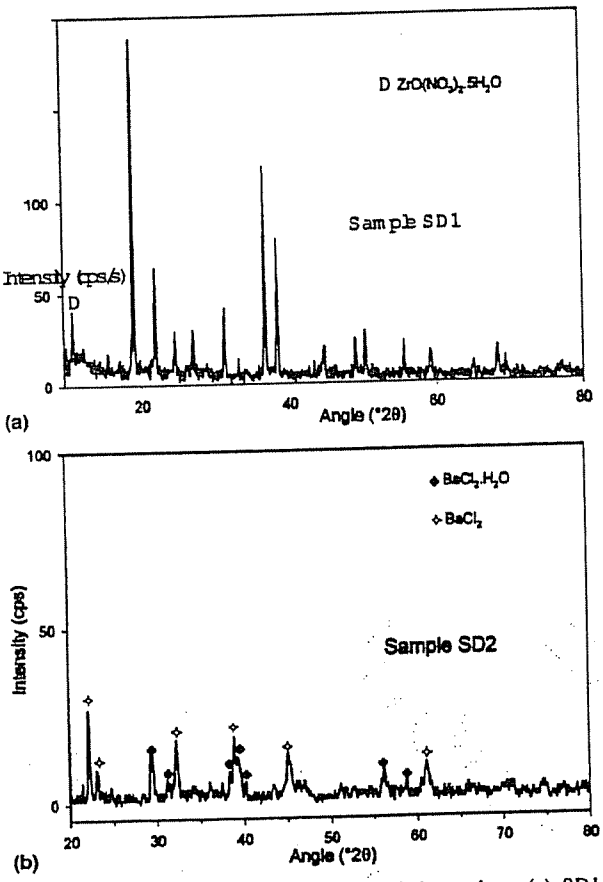

FIG. 1. XRD patterns of the as-spray-dried powders: (a) SD1 and (b) SD2.

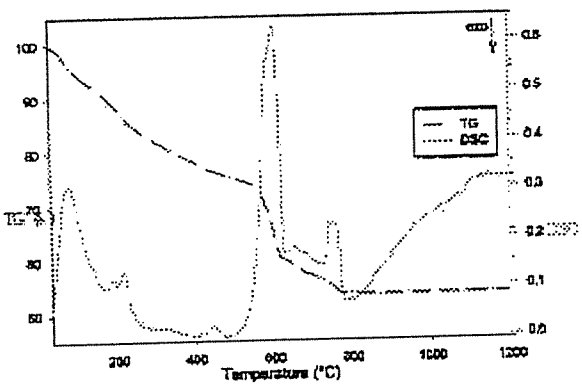

FIG. 2. TGA/DSC curve of the spray-dried mixture of nitrates (SD1).

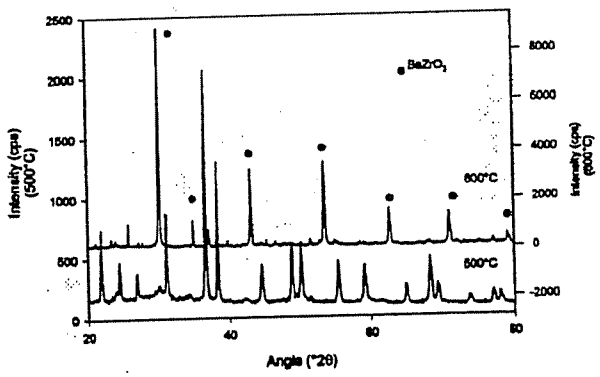

FIG. 3. XRD patterns of the spray-dried mixture of nitrates for 2 h at 500 and 600 °C.

600 °C. The weight loss around 700 °C is assigned to the loss of residual CO_2. The intensity of the x-ray pattern measured in the same conditions strongly increases when the calcination temperature goes from 500 to 600 °C. This is due to the crystallization of the barium zirconate corresponding to the broad endotherm centered around 600 °C. It is important to note that the concomittant melting of $Ba(NO_3)_2$ at 592 °C may contribute to the width of this endotherm.[18]

2. $BaZrO_3$ from the acetates solution SD3

The dissolution of zirconium carbonate in acetic acid leads to the formation of a diacetatozirconyl salt, which does not crystallize but is known to form an amorphous phase. The spray drying of the so-called acetate solution (SD3) indeed gives a solid amorphous to x-rays. However, the infrared (IR) spectrum of the spray-dried precursor is typical of acetate salts (Fig. 4). The thermal decomposition of the acetate mixture to form the barium zirconium oxide proceeds in three steps (Fig. 5). The weight loss below 250 °C is assigned to the loss of residual water molecules. Between 250 and 400 °C, the decomposition of the acetates gives rise to the formation of barium carbonate and is marked by the exothermic peak centered around 335 °C. The solid heated at 350 °C for 2 h is still amorphous to x-rays. On the corresponding IR spectrum the appearance of barium carbonate is deduced from the very sharp peak at 858 cm^{-1}, and the bands at 1058 cm^{-1}. However, the bands typical for acetate are still present (Fig. 4). After heat treatment at 400 °C for 2 h, the IR spectrum shows only the carbonate bands. The evolution of the reaction is deduced from the IR spectra. Around 350 °C, $Ba(ac)_2$ partially decomposes to $BaCO_3$. This decomposition is completed at 400 °C. Than, the $BaCO_3$ reacts with the zirconium amorphous phase to form $BaZrO_3$. The XRD pattern of the spray-dried powder calcined at 500 °C for 2 h corresponds to a pure $BaZrO_3$ phase. Remarkably, no important DSC peak

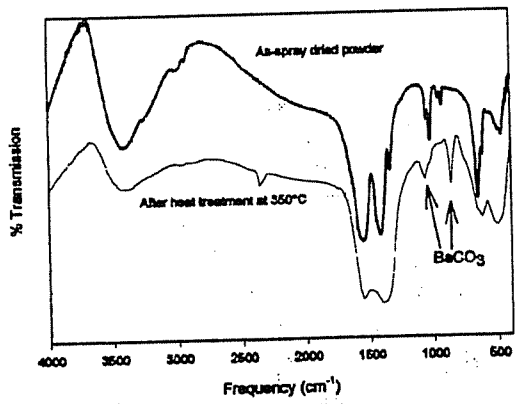

FIG. 4. IR spectrum of the as-spray dried mixture of acetates salts (SD3) and the precursor powder heat-treated at 350 °C for 2 h.

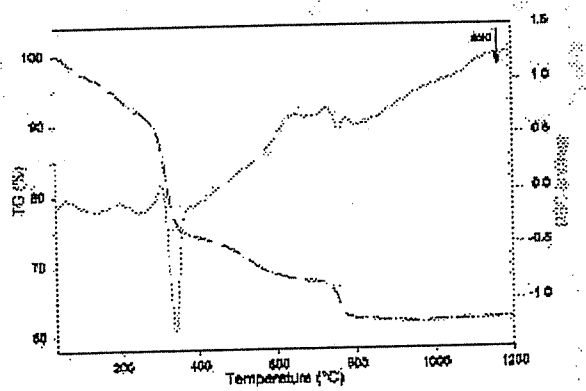

FIG. 5. TGA/DSC curve of the spray-dried mixture of acetates (SD3).

is observed between 400 and 800 °C (Fig. 5). The absence of a clear endotherm for the formation of $BaZrO_3$ may be of thermochemical origin. The reaction taking place may be written as follows:

$$BaCO_3 + ZrO_2 \rightarrow BaZrO_3 + CO_2 \quad . \qquad (1)$$

In comparison, when nitrates salts are used the reaction proceeds as follows:

$$Ba(NO_3)_2 + ZrO_2 \rightarrow BaZrO_3 + 2\ NO_2 + \tfrac{1}{2}O_2 \quad , (2)$$

with ZrO_2 in an amorphous state in both cases.

Assuming that the enthalpy of formation of amorphous ZrO_2 is equal to the enthalpy of formation of monoclinic ZrO_2, it is possible to calculate the enthalpy associated to reactions (1) and (2). The enthalpy of the reaction (1) is equal to 144 kJ/mol, whereas a value of 380 kJ/mol is calculated for Eq. (2).[18] The difference in the DSC curves of reactions (1) and (2) around 500 °C may thus reasonably be related to the difference in the enthalpy of formation of CO_2 and NO_2, respectively.

3. $BaZrO_3$ from the chlorides solutions SD2 and SD4

When chlorides are involved in the reaction (SD2, SD4), it is difficult to determine from the thermal analysis the formation temperature of the $BaZrO_3$ phase. Moreover, even if barium is introduced as nitrate, barium chloride forms due to the simultaneous decomposition of the zirconyl chloride. The barium chloride is still detected by XRD in powders calcined at temperature as high as 1000 °C. A TGA/DSC analysis of barium chloride dihydrate confirmed the stability of barium chloride up to 1000 °C. The use of chlorides as starting materials requires a washing step, and chlorides should therefore be avoided in the perspective of a fast, simple, and reproducible process to prepare barium zirconate powders.

B. Microstructural characterization

The powders obtained by the spray-drying process have a characteristic spherical shape. The size distribution is large with particles ranging from 1.5 to 15 μm. After calcination the particles are well-agglomerated.

1. Powders from the nitrate solution SD1

The spray-dried powders of nitrates mixture are characterized by a rather large size distribution of spherical particles. After calcination at 800 °C for 12 h, the particles are not spherical anymore but tend to become polyhedral (Fig. 6). The granulometric analysis of the powder gives $d(0.5) = 5.7$ μm, which corresponds to the mean size of the agglomerates. The particle-size distribution is characterized by three peaks (Fig. 7). The first peak is due to the primary particles. The second and the third peaks correspond to agglomerates.

2. Powders from the acetates solution SD3

The as-sprayed acetate mixture is characterized by the presence of two types of particles: spherical smooth particles and shriveled-up particles (see Fig. 8). The microstructure of the SD3 powder after calcination is very similar to the one observed before calcination (Fig. 8); i.e., no particular evolution is observed between as-sprayed and calcined powders. A very large size distribution can be deduced from the granulometric curve presented in Fig. 9. Primary particles with a characteristic size lower than 1 μm are clearly observed in the scanning electron photomicrograph presented in Fig. 8. These small shriveled-up particles have a tendency to agglomerate with larger smoother ones. The $d(0.5)$ deduced from Fig. 9 is 8.1 μm, which is characteristic of the large spherical particles. Small and large particles tend to deagglomerate very easily under low-energy sonication, even if a small bump is clearly visible in the granulometric curve at around 70 μm.

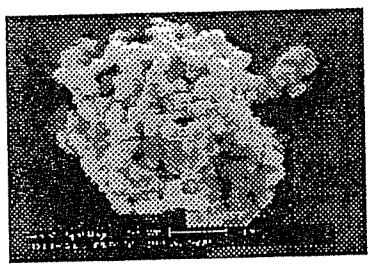

FIG. 6. Electron photomicrographs of the spray-dried mixture of nitrates calcined at 800 °C for 12 h (SD1).

3. Powders from the chlorides solution SD2

Figure 10 is a scanning electron photomicrograph of the powders obtained by calcination of the SD2 batch at 1000 °C for 12 h. The particles are spherical, and they have a mean diameter close to 0.3 μm, but they are well agglomerated. As can be seen in Fig. 10, some bigger crystals can be observed near the small, round-shaped particles of barium zirconate. These crystals are zirconium rich phases as deduced from energy dispersive x-ray (EDX) analysis but are not detected by XRD analysis. The presence of zirconium-rich phases may be explained by a leaching of the barium ions during the washing step. The inhomogeneity of the powders obtained when starting from chlorides is another reason why using these salts as precursors has not been recommended.

C. Effect of fuel addition

The presence of an organic fuel has a direct influence on the formation temperature of the barium zirconium phase and on the morphology of the calcined particles. By comparison with Fig. 2, Fig. 11 shows that the presence of a fuel reduces the temperature of formation of barium zirconate by 200 °C.

It is important to recall that the exothermic character of the reaction is not reflected in the thermogravimetric analysis due to the slow heating rate applied during the thermogravimetric measurements.

The fuel oxidation has a marked effect on the morphology of the final powder. The formation of cubic particles is clear and generalized to all the particles. The spherical spray-dried particles undergo a fragmentation into small cubes upon calcination. The cubic shape is associated with the symmetry of the perovskite unit cell. The conditions provided by the combustion technique seem to be suitable for the growth of microcrystalline

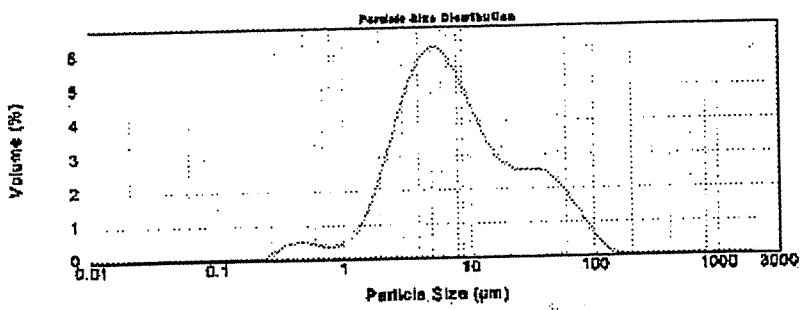

FIG. 7. Particle-size distribution of SD1 powder calcined at 800 °C for 12 h.

barium zirconate. The granulometric analysis of this powder gives a $d(0.5)$ of 1.6 μm, which is the smallest value observed (Fig. 13). The spherical agglomerates F12,F13 presented in Fig. 12(b) are thus easily broken by low-energy sonication and contribute as a very small shoulder in the size distribution curve. The addition of the fuel thus has a positive effect on the morphology and size distribution of the powder.

D. Sintering behavior

For performing dilatometric measurements, rods 25 mm long were isostatically pressed at 220 MPa for 2 h. The sintering behavior of the powders prepared using chlorides precursors was not studied due to the inhomogeneity of the final powders as indicated above. F14 Figure 14 shows the percentage of shrinkage versus temperature.

The sintering behavior of the powders depends on the nature of the precursor powders. The $BaZrO_3$ powder prepared by spray-drying and calcination of a mixture of barium acetate and zirconyl acetate (SD3) shows a reduced shrinkage of 2% at 1400 °C. The shrinkage of this powder begins at 1200 °C, i.e., the highest temperature observed for the barium zirconate powder obtained by spray-drying. The samples SD1 and SD5 on one hand, and SD6 and SD7 on the other hand, have a similar behavior. For clarity, the curves corresponding to SD1 and SD6 are not reported. From the comparison of the sample containing (SD6 and SD7) or not containing the organic fuel (SD1 and SD5), it appears that the shrinkage is greater for the sample prepared in the absence of fuel; in this case the shrinkage even overran the maximum value recorded by the apparatus (plateau from 1300 °C indicated in Fig. 14). In both cases, the onset of the shrinkage arises at 1000 °C.

FIG. 10. Electron photomicrographs of the powder calcined at 1000 °C/12 h (SD2).

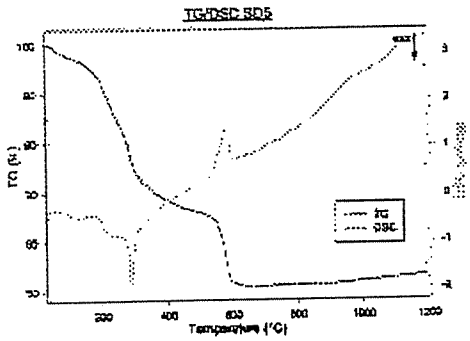

FIG. 11. TGA/DSC curve of the as-spray dried mixture of nitrates in the presence of oxalyl dihydrazide

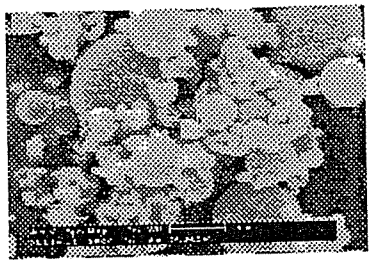

FIG. 8. Electron photomicrographs of the as-spray-dried mixture of acetates (SD3).

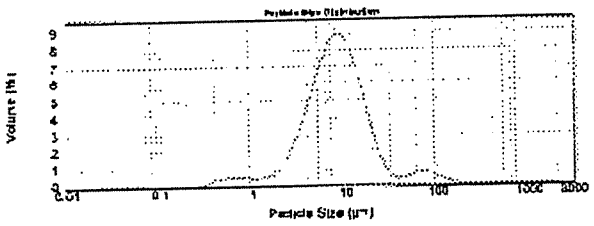

FIG. 9. Particle-size distribution of SD3 powder calcined at 800 °C for 12 h.

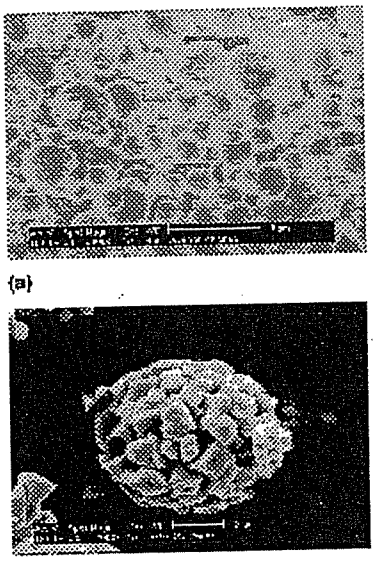

FIG. 12. Electron photomicrograph of (a) the as-spray-dried powder SD7 and (b) the same powder calcined at 800 °C for 12 h.

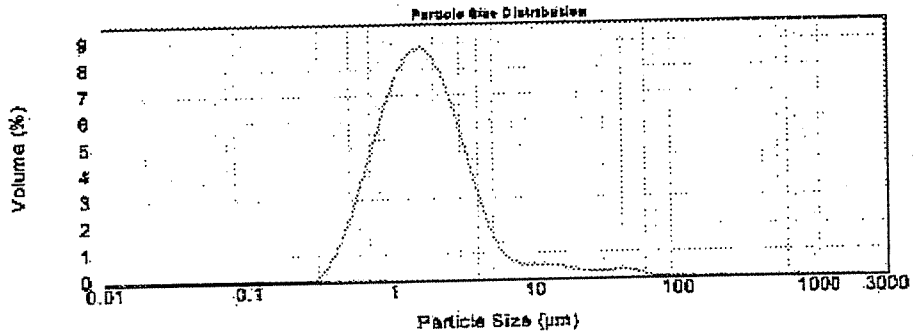

FIG. 13. Particle-size distribution of the SD7 powder calcined at 800 °C for 12 h.

Scanning electron microscopy analyses were performed on fractured parts of SD3, SD5, and SD7 samples after dilatometric measurements to investigate their sintering behavior. The results are presented in Fig. 15(a)–15(c), F15 respectively, for SD3, SD5, and SD7 samples. Solid-state sintering mechanisms were taken into account in each case. Recall that the powders obtained by spray drying are most often "low bulk density powders" due to the formation of hollow particles.[19] This is certainly the case when acetates are used as precursors (see Fig. 8, sample SD3). The shrinkage undergone by these powders is thus the lowest. Sample SD3 [see Fig. 15(a)] is effectively characterized by a large grain size and a relatively high porosity. In the SD5 and SD7 powders, the spray-dried spheres are not well preserved upon calcination, leading to a higher shrinkage during the dilatometric measurements. The SD5 sample exhibits a higher sinter activity than SD7 sample. In the case of the SD7 sample, the low shrinkage observed for the powder synthesized in the presence of a fuel may be explained by the occurrence of less reactive large cristalline fragments in sinter-SD7 powder [see Figs. 8 and 15(c)]. The presence of the fuel leads to well-crystallized agglomerated powders that are thermodynamically more stable than round less-crystalline particles. The system is less likely to rearAU3 range by itself so a higher sintering temperature is required for densification. The high crystallinity of SD7 powders and their tendency to form fragments are thus believed to be partially responsible for the poor sinterability leading to a lower final density.

The effect of agglomerates of powder particles on the sintering characteristics of compacts is thus to reduce the final density. Density achieved depends strongly on the size and packing of agglomerates, so an increased in the grinding time of the powders generally causes increased densification rates. A very homogeneous and uniform distribution of fine particles in the green state of powder compacts is thus necessary to achieve good sintering properties. Under ideal conditions, a ceramic powder-compaction process would produce a defect-free, high-density compact that shrinks uniformly during sintering. However several obstacles (including non-spherical particles and aggregates, as well as large particle size distribution) prevent this idealized situation and introduce defects. A controlled synthetic processes producing well defined systems must account for such irregularities. This is particularly true when compacts made from spray-dried powders are used.

The density of the samples after the dilatometric measurements were determined using Archimedes' principle in water. The highest density, as expected, was observed for sample SD5. However, the final density corresponds to 91% of theoretical density of $BaZrO_3$. Thus, the removal of porosity is probably a primary goal. Nevertheless, to minimize the size and concentration of pores in a compact remains a very complicated task we believe that this density may be increased by a prolonged heating treatment at 1300 or 1400 °C, as it is clear from the dilatometric measurements that the shrinkage was not completed.

It is also interesting to note that when the samples are calcined at 800 °C before shaping, the samples fracture frequently during the dilatometric measurement. For powder calcined at higher temperature (e.g., 1000 °C),

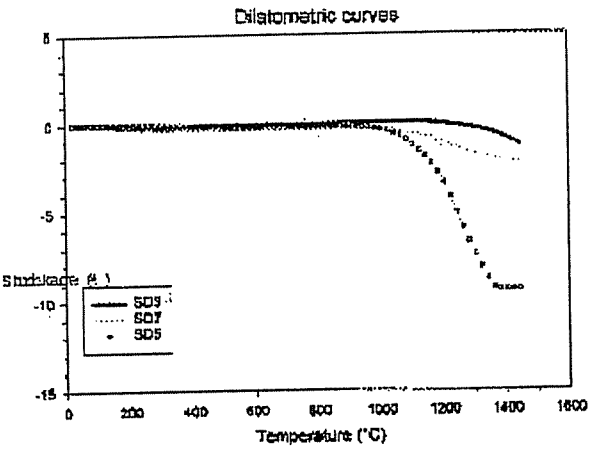

FIG. 14. Linear shrinkage of the $BaZrO_3$ rods.

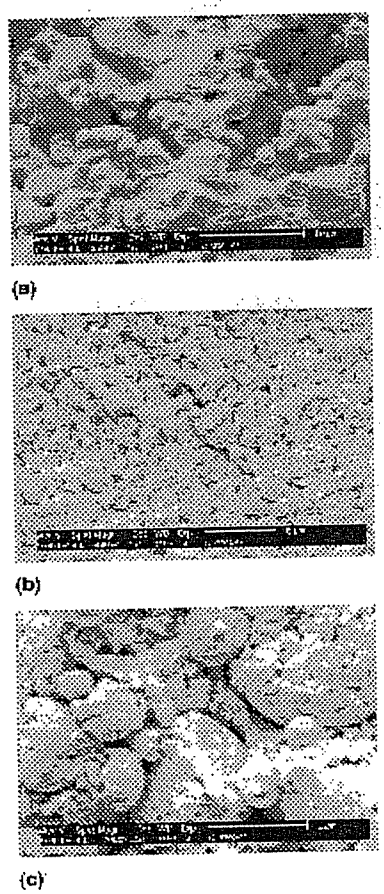

FIG. 15. (a) Electron photomicrograph of the sintered SD3 sample. (b) Electron photomicrograph of the sintered SD5 sample. (c) Electron photomicrograph of the sintered SD7 sample.

this is not observed. This breaking might be due to the presence of microstresses in the powders or to the presence of residual adsorbed gas, which are removed by that calcination at higher temperatures.[20]

IV. CONCLUSIONS

The spray-drying process enables control of the final morphology and size distribution of the powders. It also enables a fast synthesis process starting from simple precursor compounds. The use of chlorides as reagent salts should be avoided because of the inhomogeneity of the powders obtained and the washing step required. When nitrates are used as precursor powders, polyhedral particles forming loose agglomerates are observed. The addition of a organic fuel to the nitrate solution leads to particles characterized by cubic morphology and a narrow particle-size distribution. The sintering behavior of the powders using nitrate salts as precursors shows the highest shrinkage. The presence of a fuel however seems to be unfavorable to the sintering and densification of the end products. The nitrates are thus particularly interesting as precursor powders for the manufacture of barium zirconate powders.

REFERENCES

1. V.Yu. Kolen'ko, A.A. Burukhin, B.R. Churagulov, N.N. Oleinikov, and A.S. Vanetsev, Inorg. Mater. **38,** 252 (2002).
2. A. Azad and S. Subramaniam, Mater. Res. Bull. **37,** 85 (2002).
3. A. Douy, Int. J. Inorg. Mater. **3,** 699 (2001).
4. N. Lecerf, S. Mathur, H. Shen, M. Veith, and S. Hufner, Scripta Mater. **44,** 2157 (2001).
5. D.N. Philips, S. Van Bruchem, I.D. Alecu, and R.J. Stead, Brit. Ceram. Proc. **61,** 135 (2000).
6. G. Taglieri, N. Tersigni, L.P. Villa, and C. Mondelli, Int. J. Inorg. Mater. **1,** 103 (1999).
7. M. Veith, S. Mathur, N. Lecerf, V. Huch, T. Decker, H. Beck, W. Eiser, and R. Haberkorn, J. Sol-Gel Sci. Technol. **17,** 145 (2000).
8. G. Pfaff and E. Merck, Mater. Lett. **24,** 393 (1995).
9. M. Rajendran and M.S. Rao, J. Mater. Res. **9,** 2277 (1994).
10. M. Leoni, M. Viviani, P. Nanni, and V. Buscaglia, J. Mater. Sci. Lett. **15,** 1302 (1996).
11. A. Erb, E. Walker, and R. Flükiger, Physica C **245,** 245 (1995).
12. K. Masters, Spray Drying Handbook (Longman Scientific and Technical, New York, 5th ed., 1991).
13. C. De Meyer, I. Van Driessche, and S. Hoste, Key Eng. Mater. **206–213,** 11 (2002).
14. I. Van Driessche, R. Mouton, and S. Hoste, Mater. Res. Bull. **31,** 979 (1996).
15. K.R. Venkatachari, D. Huang, S.P. Ostrander, W.A. Schulze, and G.C. Stangle, J. Mater. Res. **10,** 748 (1995).
16. P. Pascal, *Nouveau traité de chimie minérale* (Masson and Cie, 1963), pp. 728–729.
17. Powder Diffraction Files Nos. 06-0399 ($BaZrO_3$), 37-1413 (o-ZrO_2), and 17-0923 (t-ZrO_2) (International Centre for Diffraction Data, 1995).
18. *Handbook of Chemistry and Physics*, 64th ed. (CRC Press, 1983).
19. D. Ganguli and M. Chatterjee, in *Ceramic Powder Preparation: A Handbook*, (Kluwer Academic Publishers, Boston, MA, 1997), pp. 35–73.
20. J. Poth, R. Haberkorn, and H.P. Beck, J. Eur. Ceram. Soc. **20,** 715 (2000).

NUMBER ____ OF ____

AUTHOR QUERIES

DATE 04/25/03
JOB NAME REMAT
JOB NUMBER 64241

ARTICLE 30 (02-0446)
QUERIES FOR AUTHOR ROBERTZ ET AL.

THIS QUERY FORM MUST BE RETURNED WITH ALL PROOFS FOR CORRECTIONS

1) AU: Spell out.

2) AU: Location of manufacturer?

3) AU: Sentence correct?

4) AU: Language? Name & location of publisher?

5) AU: Location?

6) AU: Editors?